Available online at www.sciencedirect.com

ScienceDirect

Journal of Solid State Chemistry 180 (2007) 1943–1948

JOURNAL OF SOLID STATE CHEMISTRY

www.elsevier.com/locate/jssc

Synthesis, structure, and properties of the first trimetallic phosphate $[Ni(H_2O)_4]Cd(VO)(PO_4)_2$ with neutral 3-D pillared-layer framework

Shu-Fang Zhang[a], Guang-Zhen Liu[b], Shou-Tian Zheng[a], Guo-Yu Yang[a,*]

[a]State Key Laboratory of Structural Chemistry, Fujian Institute of Research on the Structure of Matter, Chinese Academy of Sciences, Fuzhou, Fujian 350002, China
[b]Department of Chemistry, Luoyang Normal University, Luoyang 471022, China

Received 6 March 2007; received in revised form 20 April 2007; accepted 30 April 2007
Available online 6 May 2007

Abstract

Hydrothermal reactions of $VOSO_4 \cdot 3H_2O$, $CdAc_2 \cdot 2H_2O$, $NiCl_2 \cdot 6H_2O$, H_3PO_4, and H_2O yield the first example of trimetallic phosphate materials, $[Ni(H_2O)_4]Cd(VO)(PO_4)_2$ **1**. The single-crystal X-ray diffraction shows that its structure consists of Cd/V/O binary metal oxide lamellas decorated by PO_4 tetrahedra, which are further pillared by $NiO_2(H_2O)_4$ octahedra to generate a neutral 3-D framework containing two intercrossing 8-MR channels where the coordinated water molecules protrude into. Thermal and magnetic behaviors of this material were also measured. Crystal data: $CdNiVP_2O_{13}H_8$, orthorhombic *Ibca* (No.73), $a = 7.1307(2)$ Å, $b = 18.6248(3)$ Å, $c = 14.8046(2)$ Å, $V = 1966.17(7)$ Å^3, $Z = 8$.

Keywords: Trimetallic phosphate; Hydrothermal synthesis; Crystal structure; Open framework

1. Introduction

Amongst the variety of microporous compounds, those of metal phosphates constitute an important family other than initial aluminosilicates. Following the discovery of Flanigen's first microporous aluminophosphates in 1982 [1], a very wide range of the transition metals (such as Sc, Ti, Zr, V, Nb, Cr, Mn, Fe, Co, Ni, Cu, Zn, Cd, etc.) and main group elements (such as B, Al, Ga, In, etc.) have been incorporated into the framework structures of such phosphate-based materials [2]. Of particular interest is that incorporation of transition metal elements may lead to new solids with interesting electrical and magnetic properties [3] other than their conventional application as absorbents, ion exchangers, and catalysts. Typically, these phosphate materials are synthesized under mild hydrothermal conditions by using organic molecules (amines, tetralkylammoniums, etc.) as templates or structure-directing agents, which interact with the inorganic frameworks through H-bonds, or as intimate structural components of these oxide composite materials.

The vanadium phosphate system, as an important family of transition metal phosphates, has attracted extensive attention due to their useful catalytic activity and intricate framework structures [4,5]. Two primary reasons account for the structural diversity of the vanadium phosphates. Firstly, vanadium may exhibit various oxidation states (V(III), V(IV), and V(V)) and flexible coordination geometries (square pyramidal, octahedral, tetrahedral, and trigonal bipyramidal). Secondly, the vanadium and phosphorus polyhedra may display variable connect fashions, such as, sharing common corners, edges or faces, and coalescent of these modes [6]. Recent catalytic studies performed in the oxide systems indicate that their performances can be improved when multicomponent catalysts with several metals are used [7,8]. In the phosphate systems, such procedures remain rare and only a small group of bi-transition-metallic phosphates are known [9–19]. Of notable examples are a series of bimetallic oxovanadium phosphates with 1-D [11,20], 2-D [11,21,22], and 3-D [22] framework structures documented by Zubieta and co-workers. However, to the best our

---

*Corresponding author. Fax: +86 591 8371 0051.
E-mail address: ygy@fjirsm.ac.cn (G.-Y. Yang).

0022-4596/$ - see front matter © 2007 Elsevier Inc. All rights reserved.
doi:10.1016/j.jssc.2007.04.019

knowledge, no work has been carried out on the synthesis of the trimetallic phosphate materials because polymetallic oxides, for example, typically exhibit one or a small number of thermodynamically stable modifications, providing a limited scope for synthetic design, though these materials may exhibit the diversified structures and unexpected functional properties different from that of the monometallic and bimetallic phosphates.

Hydrothermal route can facilitate thermodynamic limitation of a synthetic reaction to shift to kinetic control, offering a powerful tool for the design of metastable materials. In this context, we report herein mild hydrothermal synthesis of the first trimetallic phosphate $[Ni(H_2O)_4]Cd(VO)(PO_4)_2$ **1** and describe its thermal and magnetic behaviors. The unique trimetallic phosphate material consists of Cd/V/O bimetallic oxide lamellas above and below decorated by PO_4 tetrahedra, which are further pillared by $NiO_2(H_2O)_4$ octahedra to form a neutral 3-D framework containing two intercrossing 8-MR channels occluded by the coordinated water molecules.

2. Experimental section

2.1. Synthesis

The novel trimetallic phosphate $[Ni(H_2O)_4]Cd(VO)(PO_4)_2$ **1**, was prepared by employing mild hydrothermal methods. Typically, 0.20 g of $VOSO_4 \cdot 3H_2O$, 0.266 g of $CdAc_2 \cdot 2H_2O$, and 0.238 g of $NiCl_2 \cdot 6H_2O$ were dissolved in 10 mL H_2O. To this solution, 0.2 mL H_3PO_4 was added dropwise under constant stirring, and the resulting mixture, with pH value of about 4, was sealed in a Teflon-lined steel autoclave and heated at 170 °C for 3 days. After cooling to room temperature, green prism-like crystals were obtained by filtration, washed with distilled water and dried in air (52% yield based on vanadium). The ICP analysis for the product gave the contents of Cd 22.16 wt% (calcd 22.48 wt%), V 10.66 wt% (calcd 10.19 wt%), Ni 11.20 wt% (calcd 11.74 wt%) and P 12.56 wt% (calcd 12.39 wt%), indicating a Cd:V:Ni:P ratio of 1:1:1:2. IR (cm^{-1}): 1054 (s) for $\nu(P{=}O)$, 943 (s) for $\nu(V{=}O)$, and 879 (s) for $\nu(V–O–V)$.

2.2. Characterization

Infrared spectra (IR) were obtained from sample powder pelletized with KBr on an ABB Bomen MB 102 series FTIR spectrophotometer over a range 400–4000 cm^{-1} and the inductively coupled plasma (ICP) analysis was carried out on a Perkin-Elmer Optima 3300 DV spectrometer. Magnetic measurements were performed in the temperature range 5–300 K with a SQUID MPMS-7 magnetometer manufactured by Quantum Design. Background corrections for the sample holder assembly and diamagnetic components of the compound were applied. The thermogravimetric analysis (TGA) was performed on a Mettler Toledo TGA/SDTA 851e analyzer in flowing air with a heating rate of 10 °C min^{-1}.

2.3. Determination of crystal structure

Suitable single crystal of **1** with the dimensions of $0.32 \times 0.18 \times 0.12\,mm^3$ was carefully selected under an optical microscope and glued to a thin glass fiber with epoxy resin. Crystal structure determination by X-ray diffraction was performed on a Siemens SMART CCD diffractometer with graphite-monochromated Mo$K\alpha$ ($\lambda = 0.71073$ Å) radiation at room temperature. An empirical absorption correction was applied using the SADABS program [23]. The structure was solved by direct methods using SHELXS-97 [24]. The phosphorus, vanadium, nickel, and cadmium atoms were first located, and the oxygen atoms were found in the successive difference Fourier maps. The vanadium atom is disorder over three positions. The hydrogen atoms attached to the water molecules were not located. "Hydrogen"-bonding was inferred by considering the $O \cdots O$ close contacts between 2.50 and 3.22 Å. The refinements were performed against all full matrix least-squares analysis with anisotropic thermal parameters for all non-hydrogen atoms. Crystallographic data for **1** is presented in Table 1. The final atomic coordinates and the selected bond distances are listed in Tables 2 and 3, respectively. CSD 391302 contains the supplementary crystallographic data for this paper.

3. Results and discussion

3.1. Crystal structure

Single-crystal X-ray crystallography for **1** reveals that the asymmetric unit consists of 12 independent

Table 1
Crystal data and structure refinement for **1**

Empirical formula	$CdNiVP_2O_{13}H_8$
Formula weight	500.05
Crystal system	Orthorhombic
Space group	*Ibca*
a (Å)	7.1307(2)
b (Å)	18.6248(3)
c (Å)	14.8046(2)
V (Å^3)	1966.17(7)
Z	8
D_c ($g\,cm^{-3}$)	3.379
μ(Mo$K\alpha$) (mm^{-1})	5.370
θ Range (deg)	4.12–28.32
Limiting indices	$-5 \leqslant h \leqslant 9$, $-24 \leqslant k \leqslant 24$, $-19 \leqslant l \leqslant 19$
Reflection collected	7175
Independent reflections	1211 [R(int) = 0.0420]
Data/restraints/parameters	1211/0/89
Goodness-of-fit on F^2	1.014
Final R_1, wR_2 [$I > 2\sigma(I)$]	0.0413, 0.0963
R indices (all data)	0.0434, 0.0978
Largest differential peak and hole ($e\,Å)^{-3}$	1.029 and −1.629

Table 2
Final atomic coordinates ($\times 10^4$) and equivalent thermal isotropic displacement U_{eq} ($\times 10^3$ Å^2) for **1**

Atoms	x	y	z	U_{eq}[a]
Ni(1)	5000	2500	8742(1)	7(1)
Cd(1)	5162(1)	5000	7500	20(1)
V(1)	10,346(2)	4928(1)	10,004(2)	3(1)
P(1)	7455(2)	4001(1)	8656(1)	7(1)
O(1)	7190(5)	3207(2)	8769(3)	21(1)
O(2)	7732(5)	5790(2)	7350(2)	19(1)
O(3)	5690(4)	4438(2)	8928(2)	13(1)
O(4)	9172(5)	4246(2)	9182(3)	26(1)
O(5)	12,500	4581(3)	10,000	11(1)
OW2	7085(5)	1729(2)	8745(3)	23(1)
OW3	5000	2500	7368(4)	24(1)
OW1	5000	2500	10,130(4)	26(1)

[a] U_{eq} is defined as one third of the trace of the orthogonalized U_{ij} tensor.

Table 3
Selected bond length (Å) for **1**[a]

Ni(1)–OW3	2.035(5)	Cd(1)–O(3)	2.389(4)
Ni(1)–O(1)	2.043(4)	V(1)–O(5)	1.667(2)
Ni(1)–O(1)#1	2.043(4)	V(1)–O(4)	1.948(4)
Ni(1)–OW1	2.055(6)	V(1)–O(3)#6	1.969(4)
Ni(1)–OW2#1	2.067(4)	V(1)–O(4)#5	1.983(4)
Ni(1)–OW2	2.067(4)	V(1)–O(3)#7	1.998(4)
Cd(1)–O(2)#2	2.284(4)	V(1)–O(5)#5	2.226(2)
Cd(1)–O(2)#3	2.284(4)	P(1)–O(1)	1.501(4)
Cd(1)–O(2)	2.361(4)	P(1)–O(4)	1.521(4)
Cd(1)–O(2)#4	2.361(4)	P(1)–O(3)	1.552(3)
Cd(1)–O(3)#4	2.389(4)	P(1)–O(2)#4	1.552(3)

[a] Symmetry transformations used to generate equivalent atoms: #1 $-x+1$, $-y+1/2$, z; #2 $x-1/2$, $-y+1$, z; #3 $x-1/2$, y, $-z+3/2$; #4 x, $-y+1$, $-z+3/2$; #5 $-x+2$, $-y+1$, $-z+2$; #6 $-x+3/2$, y, $-z+2$; #7 $x+1/2$, $-y+1$, z.

non-hydrogen atoms, including one Cd atom, one V atom, one Ni atom, one P atom, and eight oxygen atoms, as shown in Fig. 1. All the metal atoms (Cd, Ni, and V) are situated on the crystallographic special positions and are all octahedrally coordinated. Of the three independent metal atoms, Cd and V atoms are coordinated by six framework oxygen atoms, with Cd–O and V–O distances in the range 2.284(4)–2.389(4) and 1.667(2)–2.226(2) Å, respectively, however, the Ni atom is coordinated by two framework oxygen atoms and four terminal water molecules with Ni–O distances in the range 2.035(5)–2.067(4) Å. The P atom is situated on the crystallographic general position and adopts a tetrahedral geometry with P–O distances in the range 1.501(4)–1.552(3) Å. The PO_4 tetrahedron shares the O(2)–O(3) edge with the CdO_6 octahedron, leaving remaining two oxygen atoms (O(1) and O(4)) to bridge the $Ni_2(H_2O)_4$ and VO_6 octahedra, respectively. The valence sum calculations [25,26] give oxidation states of corresponding ions, indicating the occurrence of Cd^{2+}, Ni^{2+}, V^{4+}, and P^{5+}.

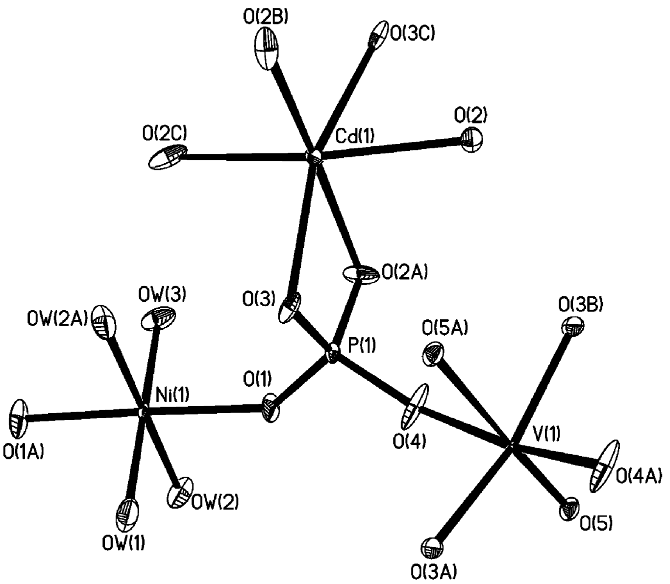

Fig. 1. Thermal ellipsoid plot (50% probability) and atom labeling scheme for asymmetric unit of **1**. Atom labels with “A” refer to symmetry-generated atoms. Two disordered positions of the V atom are omitted for clarity.

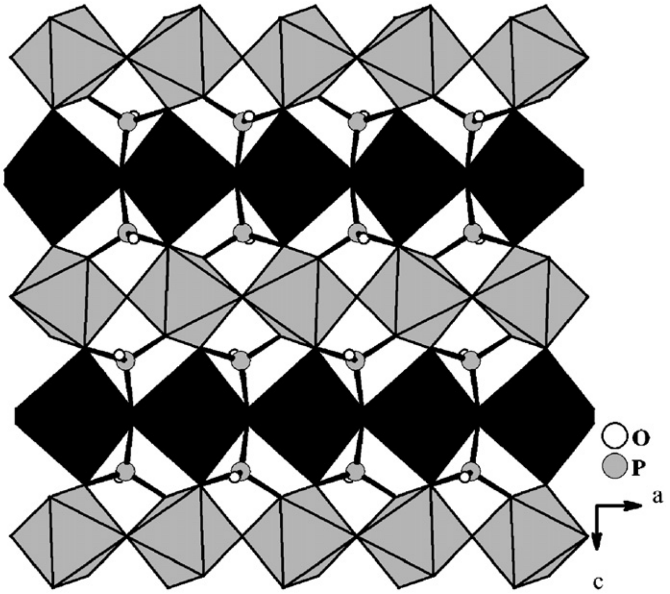

Fig. 2. View of the metal oxide lamella of Cd/V/O decocted by PO_4 tetrahedra along the [0 1 0] direction in **1**. VO_6 octahedra (gray), CdO_6 octahedra (black), and PO_4 tetrahedra (white).

The structure of **1** can be viewed as a neutral 3-D pillared-layer framework without any guest species incorporated. The layer is constructed from dense Cd/V/O oxide lamella containing 4-MRs with a PO_4 group alternately capping above and below the plane of the 4-MR (Fig. 2), which produces the rare edge-shared connections between PO_4 tetrahedra and CdO_6 octahedra. Within the lamella, a corner-shared VO_6 chain and a *trans*-edge-shared CdO_6

chain array alternately along the [0 0 1] direction and are further adhered together in the *ac* plane by sharing apical oxygen atoms of the CdO_6 and VO_6 octahedra. It is pointed that such metal oxide lamella decorated by the PO_4 tetrahedra is rather unusual in metal phosphate system. The adjacent layers are held in position by the $NiO_2(H_2O)_4$ octahedral pillars bonded to the P centers to complete the resulting 3-D architecture (Fig. 3a). Such connectivity creates two intersecting 8-MR channels parallel to the [2 0 1] and [2 0 $\bar{1}$] directions, into which the coordinated water molecules are protruded. Both pore walls of the 8-MR channels are severely staggered, which leads to only six polyhedra visible in Fig. 3a, and the opening of two 8-MR channels are built by two CdO_6, two $NiO_2(H_2O)_4$, and four PO_4 groups in the same sequence of –$NiO_2(H_2O)_4$–PO_4–CdO_6–PO_4–$NiO_2(H_2O)_4$–PO_4–CdO_6–PO_4– (Fig. 3b and c). To the best of our knowledge, this is the first example of trimetallic phosphate materials. The scarcity of the trimetallic phosphate may be attributed to the fact that few thermodynamically stable modifications of polymetallic oxides provide a limited scope for the systematic synthesis for the phosphate-based polymetallic oxides. Whereas various oxidation states, flexible coordination geometries, and variable connect fashions for vanadium account for the diversified structures of vanadium phosphates and a number of bimetallic vanadium phosphates have also been observed in the literatures. The introduction of vanadium can modify the structures of metal phosphate materials and are prone to facilitate the formation of the trimetal phosphates.

In addition, it is noteworthy that most of microporous phosphate materials consist of anionic frameworks with the template cations entrained within the channels as the counter-cations. In contrast, the framework of **1** is neutral and the synthesis is carried out under "template"-free hydrothermal conditions that is different from that of common metal phosphates where the presence of organic molecules are usually essential for the formation of resulting open-framework and the H-bonding between the framework and template is suggested to be responsible for the stabilization of open-framework structures. Within the framework of **1**, there exists some unusual intraframework H-bonding between the coordinated water molecules and lattice oxygens (O(1)) as well as between the adjacent coordinated water molecules with O···O distances in the range 2.896–3.025 Å (Fig. 4). Note that the coordinated water molecules occlude the 8-MR channels, producing a relatively dense phase; it is highly probably that these H-bonds can stabilize the framework structure of **1** in the absence of counter-cations.

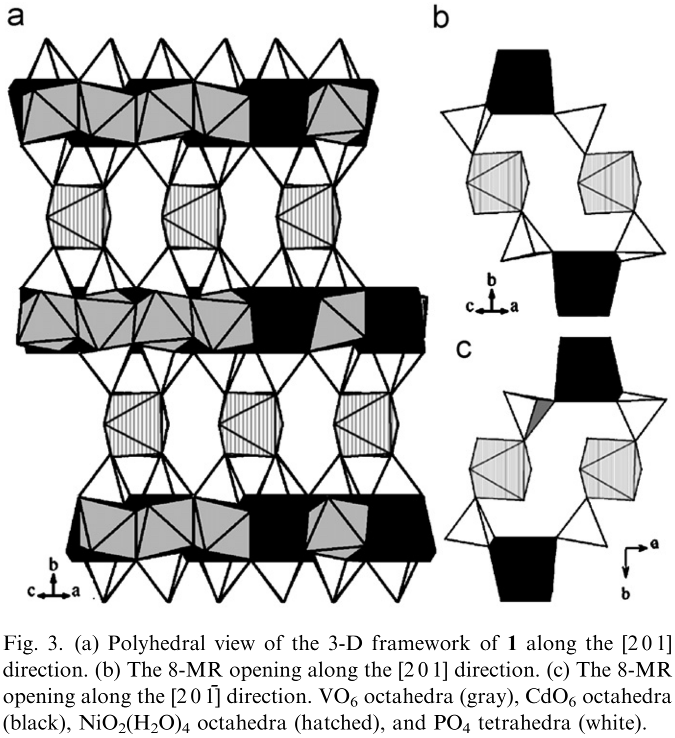

Fig. 3. (a) Polyhedral view of the 3-D framework of **1** along the [2 0 1] direction. (b) The 8-MR opening along the [2 0 1] direction. (c) The 8-MR opening along the [2 0 $\bar{1}$] direction. VO_6 octahedra (gray), CdO_6 octahedra (black), $NiO_2(H_2O)_4$ octahedra (hatched), and PO_4 tetrahedra (white).

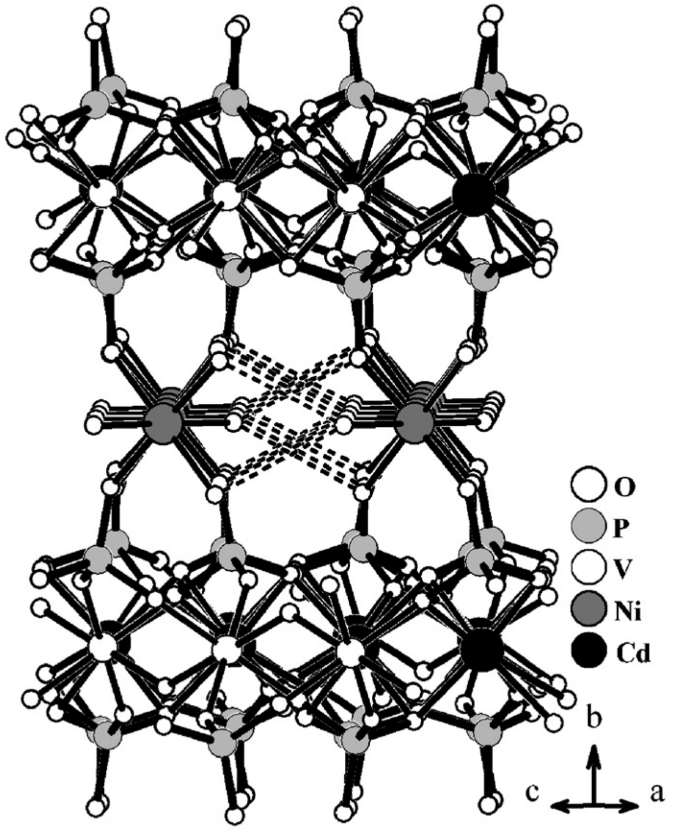

Fig. 4. Details of hydrogen bonds (dotted lines) within the framework of **1**, showing one 8-MR channel along the [2 0 1] direction.

3.2. Thermal property

The TGA curve (Fig. 5) shows **1** is thermally stable up to 200 °C. Subsequently, decomposition occurs in three steps with a total weight loss of 17.55% until 900 °C. The initial two sharp weight losses of 14.52% between 200 and 500 °C can be assigned to the release of the coordinated water molecules (calcd 14.38%). The third step with a slow

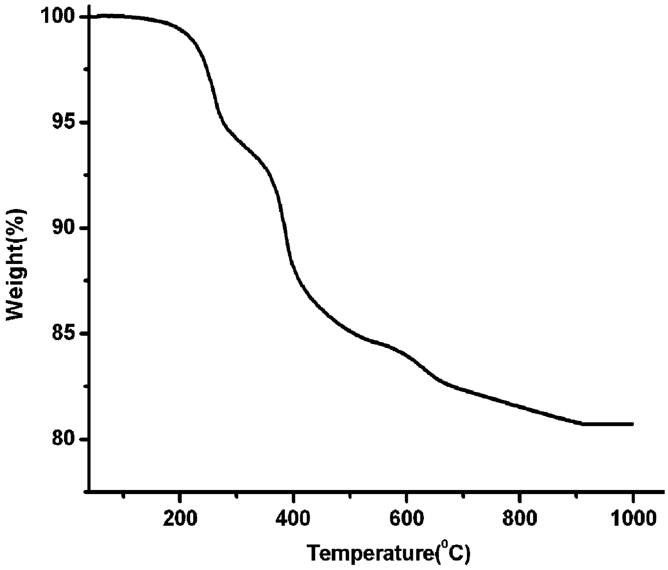

Fig. 5. TGA curves of **1**.

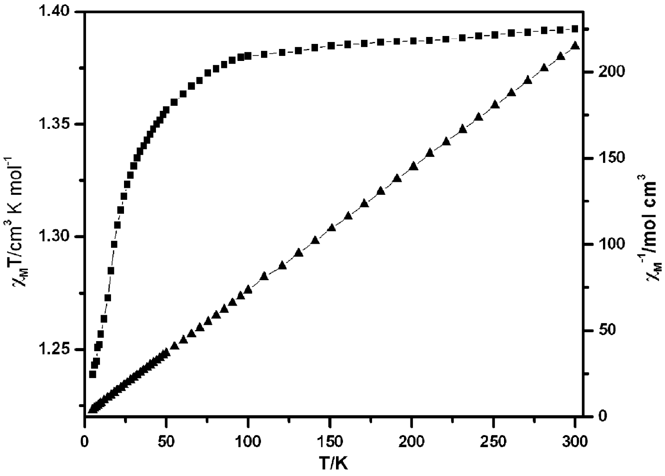

Fig. 6. Temperature dependence of $\chi_M T$ and $1/\chi_M$ for **1**.

weight loss of 3.03% between 500 and 900 °C is caused by the partial sublimation of CdO [27,28].

3.3. Magnetic property

The temperature dependence of $\chi_M T$ and $1/\chi_M$ for **1** are shown in Fig. 6. At room temperature, the effective magnetic moment determined by the equation $\mu_{\mathrm{eff}} = 2.828(\chi_M T)^{1/2}$ is $3.34\,\mu_B$, which is slightly lower than the theoretical spin-only value $3.56\,\mu_B$ expected for the combinations of one V^{4+} ($S = 1/2$, $g = 2.0$) and one Ni^{2+} ($S = 1$, $g = 2.2$). The magnetic susceptibility data can be fitted to the Curie–Weiss law $\chi_M = C/(T\text{–}\theta)$, yielding the $C = 1.396\,\mathrm{emu\,K\,mol^{-1}}$ and $\theta = -1.389\,\mathrm{K}$. The result together with the continuous decrease $\chi_M T$ values with decreasing temperature indicates that the dominant magnetic exchange interactions are antiferromagnetic.

4. Conclusions

In summary, hydrothermal synthesis of an unprecedented trimetallic phosphate with interesting structure and magnetic properties has been accomplished. Its structure consists of Cd/V/O binary metal oxide lamellas decorated by PO_4 tetrahedra, which are further pillared by $NiO_2(H_2O)_4$ octahedra to form entire 3-D framework structure containing two intercrossing 8-MR channels occluded by the coordinated water molecules. This material joins a small group of phosphates with neutral framework and represents the first example of trimetallic phosphates. It is shown that mild hydrothermal route can facilitate the self-assembly of polymetallic oxide materials. Studies on analogous polymetallic phosphate compounds of different combinations of metal ions are in progress.

Acknowledgments

This work was supported by 973 Program (No. 2006CB932900) the NNSF of China (Nos. 20473093 and 20271050), the NSF of Fujian Province (E0510030), and the Key Project from CAS (No. KJCX2-YW-H01).

References

[1] S.T. Wilson, B.M. Lok, C.A. Messina, T.R. Cannan, E.M. Flanigen, J. Am. Chem. Soc. 4 (1982) 1146.
[2] A.K. Cheetham, G. Férey, T. Loiseau, Angew. Chem. Int. Ed. 38 (1999) 3268.
[3] M. Cavellec, D. Riou, G. Férey, Inorg. Chim. Acta 291 (1999) 317.
[4] G. Centi, Catal. Today 16 (1993) 5.
[5] M.T. Sananes, G.J. Hutchings, J.C. Volta, Chem. Commun. (1995) 243.
[6] B.K. Koo, W. Ouellette, E.M. Burkholder, V. Golub, J. Zubieta, Solid State Sci. 6 (2004) 461.
[7] H. Ponceblanc, J.M.M. Millet, G. Coudurier, J.C. Védrine, in: S.T. Oyama, J.W. Hightower (Eds.), Symposium on Catalytic Selective Oxidation, ACS Symposium Series, vol. 523, American Chemical Society, Washington, DC, 1993, p. 1114.
[8] K.T. Li, N.S. Shyu, Ind. Eng. Chem. Res. 36 (1997) 1480.
[9] S. Boudin, J. Chardon, B. Raveau, Chem. Mater. 13 (2001) 4101.
[10] Z. Shi, S.-H. Feng, L.-R. Zhang, G.-Y. Yang, J. Hua, Chem. Mater. 12 (2000) 2930.
[11] R. Finn, J. Zubieta, Chem. Commun. (2000) 1321.
[12] S. Messaoudi, E. Furet, J.Y. Pivan, Chem. Mater. 16 (2004) 435.
[13] X.-M. Zhang, M.-L. Tong, S.-H. Feng, X.-M. Chen, J. Chem. Soc., Dalton Trans. (2001) 2069.
[14] E.L. Fur, R. Gautier, E. Furet, J.Y. Pivan, Inorg. Chem. 41 (2002) 4227.
[15] P. Crespoa, A. Grandin, M.M. Borel, A. Leclaire, B. Raveau, J. Solid State Chem. 105 (1993) 307.
[16] S. Boudin, A. Grandin, M.M. Borel, A. Leclaire, B. Raveau, J. Solid State Chem. 110 (1994) 43.
[17] A. Leclaire, A. Grandin, J. Chardon, M.M. Borel, B. Raveau, Eur. J. Solid State Chem. 30 (1993) 393.
[18] A. Leclaire, J. Chardon, A. Grandin, M.M. Borel, B. Raveau, Eur. J. Solid State Chem. 30 (1993) 461.
[19] S. Boudin, A. Grandin, M.M. Borel, A. Leclaire, B. Raveau, J. Solid State Chem. 111 (1994) 365.
[20] R.C. Finn, J. Zubieta, J. Chem. Soc., Dalton Trans. (2002) 856.
[21] R. Finn, J. Zubieta, J. Chem. Soc., Dalton Trans. (2000) 1821.
[22] R. Finn, R. Lam, J. Greedan, J. Zubieta, Inorg. Chem. 40 (2001) 3745.

[23] G.M. Sheldrick, A Program for the Siemens Area Detector Absorption correction, University of Göttingen, 1997.

[24] G.M. Sheldrick, SHELXS97 Program for Solution of Crystal Structures, University of Göttingen, Göttingen, Germany, 1997; G.M. Sheldrick, SHELXL97 Program for Solution of Crystal Structures, University of Göttingen, Germany, 1997.

[25] I.D. Brown, D. Altermatt, Acta Crystallogr. B 41 (1985) 244.

[26] M. O'Keeffe, A. Navrotsky, Structure and Bonding in Crystals, Vol. II, Academic Press, New York, 1981, p. 18.

[27] R. Vaidhyanathan, S. Natarajan, C.N.R. Rao, Inorg. Chem. 41 (2002) 5226.

[28] Y.-Q. Sun, J. Zhang, G.-Y. Yang, J. Coord. Chem. 57 (2004) 1299.